

in many attempts to grow large single crystals of any of the compounds described in this paper. Measurements on such crystals would provide more information on what is happening in these systems. Specific heat studies are also required.

We have tried a number of methods but have never succeeded in growing single crystals of $[\text{Cr}(\text{C}_5\text{H}_5\text{NO})_6](\text{ClO}_4)_3$. This stands in marked contrast to the great success we have had in preparing single crystals of the pyridine *N*-oxide complexes of the divalent iron series ions. Nevertheless we measured the susceptibility of a polycrystalline sample of this material and find that it obeys the Curie-Weiss law over the temperature interval 1.2-4.2 K with a *g* value of 1.965 and a θ of -0.03 ± 0.05 K. In view of the other results reported here, it was decided that this compound probably would not order at an accessible temperature, and so no further measurements were made. Again this behavior stands in stark contrast to that observed with the other pyridine *N*-oxide complexes, as well as with $[\text{Gd}(\text{C}_5\text{H}_5\text{NO})_8](\text{ClO}_4)_3$.³³

Acknowledgment. This research was supported in Chicago by the Solid State Chemistry Program, Division of Materials Research, National Science Foundation, through Grant DMR-7906119, and in Barcelona by the "Comisión Asesora de Investigación Científica y Técnica" and the "Generalitat de Catalunya". We thank Hans van Duynveldt for useful comments on the manuscript.

Registry No. $[\text{Co}(\text{NH}_3)_6][\text{Cr}(\text{CN})_6]$, 38670-48-3; $[\text{Cr}(\text{H}_2\text{O})(\text{N}-\text{H}_3)_5][\text{Co}(\text{CN})_6]$, 62534-93-4; $[\text{Co}(\text{H}_2\text{O})(\text{NH}_3)_5][\text{Cr}(\text{CN})_6]$, 60897-44-1; *cis*- $[\text{Cr}(\text{H}_2\text{O})_2(\text{NH}_3)_4][\text{Co}(\text{CN})_6]$, 86668-08-8; $[\text{Cr}(\text{H}_2\text{O})(\text{NH}_3)_5](\text{CuCl}_2)$, 86646-30-2; $[\text{Cr}(\text{H}_2\text{O})(\text{NH}_3)_5][\text{Cr}(\text{NCS})_6]$, 86646-31-3; $[\text{Cr}(\text{H}_2\text{O})(\text{NH}_3)_5][\text{Cr}(\text{CN})_6]$, 75058-08-1; $[\text{Cr}(\text{urea})_6][\text{Cr}(\text{CN})_6]$, 23540-67-2; $[\text{Cr}(\text{urea})_6][\text{Cr}(\text{NCS})_6]$, 27933-99-9; $[\text{Cr}(\text{en})_3][\text{Cr}(\text{CN})_6]$, 23540-71-8; $[\text{Cr}(\text{Me}_2\text{SO})_6][\text{Cr}(\text{CN})_6]$, 86646-32-4.

(33) Carlin, R. L.; Burriel, R.; Mennenga, G.; de Jongh, L. J., to be submitted for publication.

Contribution from the Departments of Chemistry, University of Denver, Denver, Colorado 80208, and University of Colorado at Denver, Denver, Colorado 80202

Metal-Nitroxyl Interactions. 31. Single-Crystal EPR Spectra of a Spin-Labeled Vanadyl Porphyrin

REDDY DAMODER, KUNDALIKA M. MORE, GARETH R. EATON,* and SANDRA S. EATON

Received January 21, 1983

Single-crystal EPR spectra have been obtained for a spin-labeled vanadyl porphyrin doped into zinc tetraphenylporphyrin. Four conformations of the molecule were observed. The dependence of the spin-spin splittings on the orientation of the crystal in the magnetic field was analyzed to obtain the isotropic exchange and anisotropic dipolar contributions to the spin-spin interaction. The interspin distance, *r*, ranged from 9.8 to 13.6 Å. The exchange interaction was found to be small, with values of the coupling constant, *J*, ranging from -3 to $+4 \times 10^{-4}$ cm⁻¹. The *g* and *A* values for the vanadyl electron in the spin-labeled complex agreed well with those obtained for vanadyl tetraphenylporphyrin doped into the same host.

Introduction

The understanding of spin-spin interaction between non-equivalent unpaired electrons is important to a variety of chemical and biochemical problems. Radical pairs have been observed in the EPR spectra of several photochemical systems.¹ Spin-spin interaction between a cobalt(II) center and a free radical has been detected in vitamin B₁₂ coenzyme systems.²⁻⁴ Nitroxyl spin labels attached to paramagnetic biomolecules⁵ can exhibit spin-spin interaction.⁶ In these and other similar cases, considerable insight into the structure of the system can be obtained by an analysis of the spin-spin interaction. In general, the interaction will consist of an anisotropic dipolar contribution and an isotropic exchange contribution. These two terms provide complementary information about the system. The magnitude of the dipolar interaction is determined by the distance between the two unpaired spins and the orientation of the interspin vector relative to the external magnetic field. When the EPR spectrum of the interacting spins includes resolved anisotropic nuclear hyperfine splitting, the orientation of the interspin vector relative to the nuclear hyperfine tensor can be obtained.⁷⁻⁹ Thus the dipolar interaction provides geometric information. The exchange interaction is dependent on the through-bond pathway between the two electrons and thus can provide information about the connectivity in the system. In addition, it is important to de-

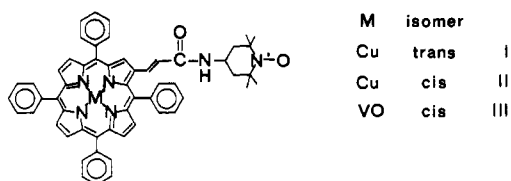
termine the conditions under which it is reasonable to assume that either the exchange or dipolar contributions would be expected to dominate the spin-spin interaction in a complex system. Elucidation of the effect of the bonding pathway on exchange is also important to an understanding of electron transport and electron polarization.

Recent results from our laboratories have shown that for spin-labeled copper(II), silver(II), and vanadyl(IV) complexes that are tumbling rapidly in solution, exchange interactions in the range of $(3-2000) \times 10^{-4}$ cm⁻¹ can be determined by analysis of the EPR spectra.^{6,10,11} Since the dipolar interaction depends on the orientation of the interspin vector relative to the magnetic field, its contribution to the spin-spin splitting

- (1) Blankenship, R. E. *Acc. Chem. Res.* **1981**, *14*, 163-170.
- (2) Schepler, K. L.; Dunham, W. R.; Sands, R. H.; Fee, J. A.; Abeles, R. H. *Biochim. Biophys. Acta* **1975**, *397*, 510-518.
- (3) Buettner, G. R.; Coffman, R. E. *Biochim. Biophys. Acta* **1977**, *480*, 495-505.
- (4) Boas, J. F.; Hicks, P. R.; Pilbrow, J. R.; Smith, T. D. *J. Chem. Soc., Faraday Trans. 2* **1978**, *74*, 417-431.
- (5) Berliner, L. J., Ed. "Spin Labeling II"; Academic Press: New York, 1979.
- (6) Eaton, S. S.; Eaton, G. R. *Coord. Chem. Rev.* **1978**, *26*, 207-262.
- (7) Eaton, S. S.; More, K. M.; Sawant, B. M.; Boymel, P. M.; Eaton, G. R.; *J. Magn. Reson.* **1983**, *52*, 435-449.
- (8) Damoder, R.; More, K. M.; Eaton, G. R.; Eaton, S. S. *J. Am. Chem. Soc.* **1983**, *105*, 2147-2153 and references therein.
- (9) Smith, T. D.; Pilbrow, J. R. *Coord. Chem. Rev.* **1974**, *13*, 173-278.
- (10) More, K. M.; Eaton, S. S.; Eaton, G. R. *J. Am. Chem. Soc.* **1981**, *103*, 1087-1090.
- (11) More, K. M.; Eaton, G. R.; Eaton, S. S. *Can. J. Chem.* **1982**, *60*, 1392-1401 and references therein.

* To whom correspondence should be addressed at the University of Denver.

is averaged to approximately zero by rapid molecular tumbling. Thus, it is necessary to use rigid-lattice spectra—powders, frozen glasses, or single crystals—to measure dipolar splittings. In the analysis of rigid-lattice spectra it is necessary to separate the dipolar and exchange contributions to the observed splittings. We have recently shown that when the exchange and dipolar contributions to the spin-spin interaction are of similar magnitude and the spectra are well resolved, it is possible to determine both the spin of the exchange coupling constant, J , and the interspin distance, r , from frozen-glass spectra of spin-labeled copper complexes.⁷ It was found that the values of J in the rigid lattice were similar in magnitude to the values observed in fluid solution.⁷ In some cases it was observed that more than one conformation of the molecule was present and that the spin-spin interaction was conformation dependent.⁷ To obtain more detailed information concerning spin-spin interactions and an unambiguous separation of the exchange and dipolar contributions to the interaction, we have studied the single-crystal EPR spectra of the spin-labeled copper complexes I and II doped into zinc tetraphenyl-



porphyrin.⁸ For both I and II, the values of r and J were obtained for four conformations of the molecule.⁸ In fluid solution it was observed that the value of J for the spin-labeled vanadyl complex III was smaller than for the analogous copper complexes I and II. It was of interest to see whether the pattern was maintained in a rigid lattice. Therefore, we have obtained single-crystal EPR spectra of III doped into zinc tetraphenylporphyrin. As part of this analysis, we also obtained single-crystal EPR spectra of vanadyl tetraphenylporphyrin doped into zinc tetraphenylporphyrin.

Experimental Section

The compounds studied here were prepared by literature methods: III,¹⁰ tetraphenylporphyrin,^{12,13} vanadyl porphyrin (VO(TPP)),¹⁴ zinc tetraphenylporphyrin (ZnTPP).¹⁴ No EPR signal was observed for ZnTPP as a powder or as a single crystal. Tetrahydrofuran (THF) was dried over potassium ribbon, distilled, and stored in the dark. EPR spectra were obtained at room temperature on a Varian E-9 spectrometer. Data were collected digitally with a Varian 620-L103 minicomputer and the CLASS language. To improve the signal-to-noise ratio of the spectra, modulation amplitudes up to half the peak-to-peak line widths were used to obtain the spectra. Although the use of such large modulation amplitudes causes slight distortion of the line shape, it should have no impact on the apparent line positions and a negligible impact on the analysis of the spectra.

Single crystals were grown by slow evaporation (3–4 days) of a solution containing a 99:1 ratio by weight of ZnTPP:III or ZnTPP:P:VO(TPP) in purified THF. Repeated recrystallization of the ZnTPP doped with III or VO(TPP) was necessary to obtain suitable crystals. The crystals used to obtain the EPR spectra were approximately $3 \times 1.5 \times 1.5$ mm.

The crystals were mounted with Dow silicone stopcock grease in a 3.5-mm segment of Wilmad synthetic quartz square-cross-section tubing (WQS-102, 2-mm i.d., 0.75-mm wall). A face of the holder was attached to the rod of a Varian E-229 one-cycle goniometer. The crystal of VO(TPP) doped into ZnTPP was oriented such that the largest face of the crystal was perpendicular to the rotation axis of the goniometer and parallel to a face of the holder and the long axis of the crystal was parallel to a second face of the holder. EPR spectra

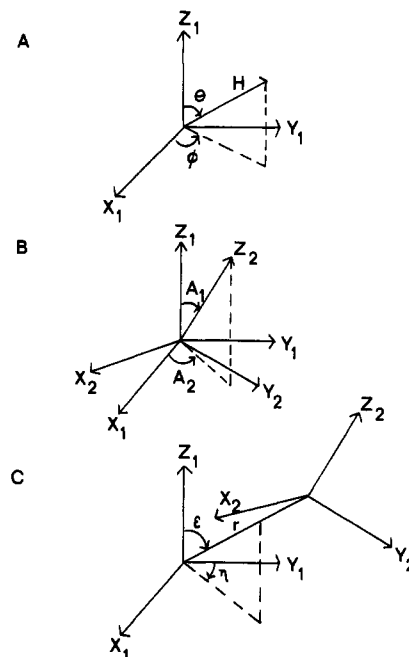


Figure 1. Definitions of the angles that relate the orientation of the magnetic field, the nitroxyl hyperfine tensor, and the interspin vector to the axes of the vanadyl hyperfine tensor (electron 1). (A) The angles θ and ϕ define the orientation of the magnetic field. (B) The angles A_1 and A_2 define the orientation of the z axis of electron 2 (nitroxyl). (C) The angles ϵ and η define the orientation of the interspin vector r . Throughout the text, r is used to denote the magnitude of the interspin vector.

were obtained at 15° intervals in this plane and in the two perpendicular planes defined by successively attaching the rod of the goniometer to the other two perpendicular faces of the holder. For the crystal of III doped into ZnTPP, the orientation of the crystal in the holder was adjusted iteratively to align the z axis of the vanadyl hyperfine tensor with the rotation axis of the goniometer. The alignment was adjusted until rotation by 180° caused little change in the vanadyl hyperfine splitting. EPR spectra were then collected at 10° intervals in this plane. The goniometer rod was then attached successively to the other two perpendicular faces of the holder, and data were collected as in the first plane. The accuracy of the rotation angles was indicated by the fact that in each plane spectra taken at 180° agreed with those at $0 \pm 1^\circ$.

Computer Simulations

The perturbation calculation used in the simulation of the spectra is similar to that described previously for the analysis of powder and single-crystal spectra of spin-labeled copper complexes.^{7,8} The Hamiltonian (eq 1) consists of terms for independent electrons 1

$$\mathcal{H} = \mathcal{H}_1 + \mathcal{H}_2 + \mathcal{H}_{\text{int}} \quad (1)$$

$$\mathcal{H}_i = \sum_{j=x,y,z} (\beta g_j S_{ij} H_j + A_j S_{ij} I_{ij}) \quad (i = 1, 2) \quad (2)$$

$$\mathcal{H}_{\text{int}} = -JS_1 S_2 + \mathcal{H}_{\text{dipolar}} \quad (3)$$

(vanadyl) and 2 (nitroxyl) as given in eq 2 and an interaction term as given in eq 3. The interaction term includes an isotropic exchange interaction and an anisotropic dipolar interaction. The symbols in eq 1–3 have their usual meanings and are discussed in detail in ref 4 and 7–9. The splitting between the single and triplet levels is J , and a negative value of J indicates an antiferromagnetic interaction. The angles that define the relative orientations of the hyperfine axes of electrons 1 and 2, the dipolar tensor, and the magnetic field direction are shown in Figure 1. In the following discussion, r is used to denote the magnitude of the interspin vector and its orientation is defined by the angles ϵ and η . The orientation dependence of the nitrogen hyperfine splitting and of the electron–electron spin–spin splitting was analyzed by using the computer program ROTAN.⁸ The EPR spectra were simulated by using the program CRYST.⁸

Simulation of the vanadyl lines in the spectra of III doped into ZnTPP indicated that the vanadyl z axis was 12° away from the z

(12) Adler, A. D.; Longo, F. R.; Finarelli, J. D.; Goldmacher, J.; Assour, J.; Korsakoff, L. *J. Org. Chem.* **1967**, *32*, 476.

(13) Rousseau, K.; Dolphin, D. *Tetrahedron Lett.* **1974**, 4251–4254.

(14) Adler, A. D.; Longo, F. R.; Kampas, F.; Kim, J. *J. Inorg. Nucl. Chem.* **1970**, *32*, 2443–2444.

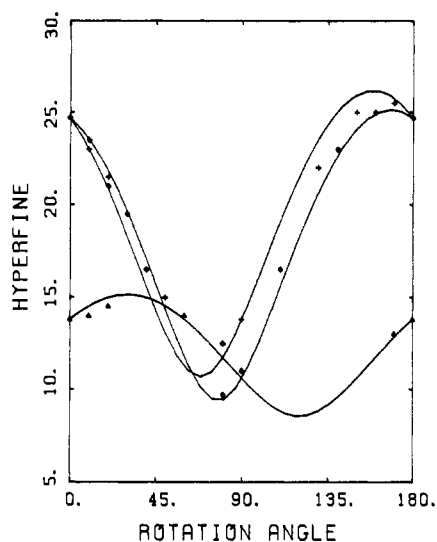


Figure 2. Plots of the orientation dependence of the nitroxyl nitrogen hyperfine splitting (in gauss) in three orthogonal planes for species 1-4 of spin-labeled vanadyl complex III doped into ZnTPP. Experimental data: (\blacktriangle) *xy* plane; (\blacklozenge) *xz* plane; (+) *yz* plane. The solid lines are the calculated curves.

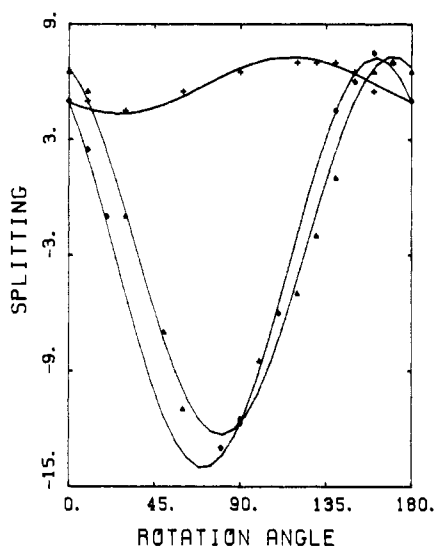


Figure 3. Plots of the orientation dependence of the spin-spin splitting (in gauss) in three orthogonal planes for species 1 of spin-labeled vanadyl complex III doped into ZnTPP. Experimental data: (\blacktriangle) *xy* plane; (\blacklozenge) *xz* plane; (+) *yz* plane. The solid lines are the calculated curves.

axis used for data collection. The plots in Figures 2-6 are given in the experimental axis system. The orientation parameters obtained by simulation of these plots were transformed to the vanadyl axis system. The parameters cited in the text and used in the simulations of the spectra are relative to the vanadyl axes. When VO(TPP) or III was doped into ZnTPP, the orientation of the vanadyl *z* axis relative to the faces of the crystal was about the same as was observed for the copper *z* axes of I and II doped into ZnTPP. Thus, the orientations of the porphyrin plane in the host lattice are about the same for the vanadyl and copper complexes and are not changed by attachment of the nitroxyl side chain.

Analysis of EPR Spectra

Weak electron-electron spin-spin interaction is expected to consist of an isotropic exchange contribution and an anisotropic dipolar interaction. The resulting EPR spectra have been referred to as AB patterns^{2-4,6} by analogy with high-resolution NMR.¹⁵ As a result

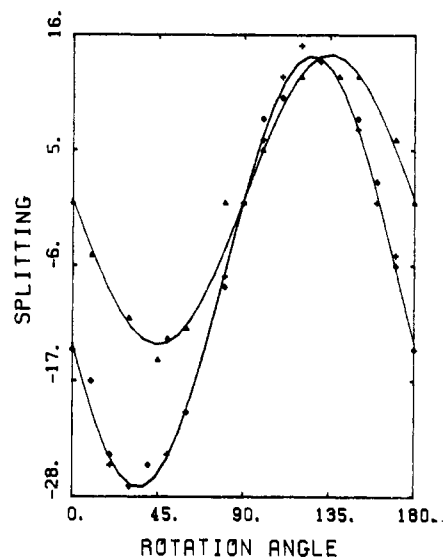


Figure 4. Plots of the orientation dependence of the spin-spin splitting (in gauss) in three orthogonal planes for species 2 of spin-labeled vanadyl complex III doped into ZnTPP. Experimental data: (\blacktriangle) *xy* plane; (\blacklozenge) *xz* plane; (+) *yz* plane. The solid lines are the calculated curves.

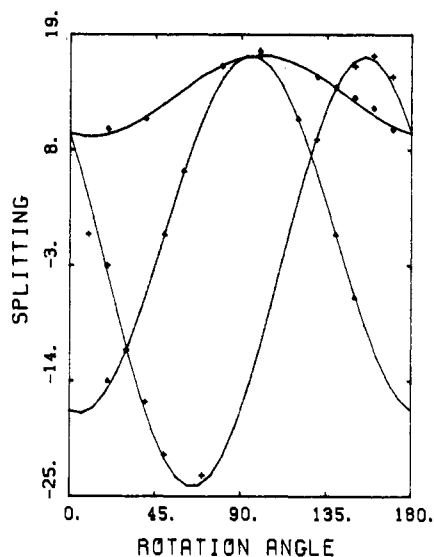


Figure 5. Plots of the orientation dependence of the spin-spin splitting (in gauss) in three orthogonal planes for species 3 of spin-labeled vanadyl complex III doped into ZnTPP. Experimental data: (\blacktriangle) *xy* plane; (\blacklozenge) *xz* plane; (+) *yz* plane. The solid lines are the calculated curves.

of the interaction, each of the hyperfine lines for each of the electrons is split into a doublet. For the spin-labeled vanadyl complex, there are theoretically 432 vanadyl lines and 432 nitroxyl lines in the spectrum if the effects of the vanadyl nuclear spin, the spins of the porphyrin nitrogens, the nitroxyl nitrogen nuclear spin, and the electron-electron spin-spin interaction are included. It is assumed that only $\Delta m_l = 0$ transitions are observed. However, the splitting of the nitroxyl lines by the vanadyl nuclear spin and by the spins of the porphyrin nitrogens was too small to be observed, so the nitroxyl portion of the AB patterns was an apparent six-line pattern. In the spectra of VO(TPP), there was partially resolved nitrogen hyperfine splitting on each of the eight vanadyl hyperfine lines. In the spectra of the spin-labeled vanadyl porphyrin III, the electron-electron spin-spin splittings were smaller than the apparent line widths due to the nitrogen hyperfine splittings, so the vanadyl lines were eight multiplets with poorly resolved splittings. Therefore, the analysis of the electron-electron spin-spin interaction in III was based on the nitroxyl lines in the spectra. The computer simulations based on the analysis of the nitroxyl lines were consistent with the absence of resolved spin-spin splitting of the vanadyl lines.

(15) Abraham, R. J. "The Analysis of High Resolution NMR Spectra"; Elsevier: Amsterdam, 1971; Chapter 3.

Table I. Spin-Hamiltonian Parameters for the Vanadyl and Nitroxyl Electrons in Spin-Labeled Porphyrin III

electron	species	g_{xx}	g_{yy}	g_{zz}	A_{xx}^a	A_{yy}^a	A_{zz}^a
vanadyl ^{b,c}	1-4	1.9837	1.9837	1.9635	56	56	158
nitroxyl	1, 3, 4	2.0075	2.0063	2.0040	10.5	8.0	25.5
nitroxyl	2	2.0075	2.0063	2.0030	10.5	8.0	27.0

^a In units of 10^{-4} cm^{-1} . ^b The same g and A values were observed for VO(TPP) doped into ZnTPP. ^c The apparent nitrogen hyperfine coupling constants along the x , y , and z axes of the vanadyl ion were 2.3, 2.3, and $2.6 \times 10^{-4} \text{ cm}^{-1}$.

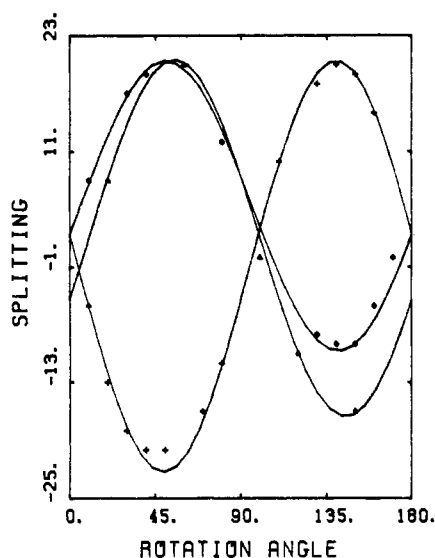


Figure 6. Plots of the orientation dependence of the spin-spin splitting (in gauss) in three orthogonal planes for species 4 of spin-labeled vanadyl complex III doped into ZnTPP. Experimental data: (\blacktriangle) xy plane; (\blacklozenge) xz plane; ($+$) yz plane. The solid lines are the calculated curves.

The number of lines in the nitroxyl regions of the spectra of III indicated that more than one AB pattern was present. The vanadyl lines indicated that the orientation of the z axis of the vanadyl A tensor was the same for all the components of the spectra. Comparison of the spectra obtained in the three orthogonal planes showed that the multiple AB patterns did not result from sites that were related by rotation around the vanadyl z axis or by reflection in the porphyrin plane. Thus it was necessary to treat the spectra as the sum of the contributions from species with different orientations of the interspin vector relative to the vanadyl tensor and with different values of r and J .

The assignment of the lines in the spectra to AB patterns was performed as previously reported for spin-labeled copper complexes I and II.⁸ The population of species 1 was greater than that of the other species and its lines had the narrowest line widths so it gave the prominent lines at most orientations of the crystal. Since the electron-electron spin-spin splitting for species 1 was smaller than the nitrogen hyperfine splitting at most orientations of the crystal, the anisotropy of the nitroxyl nitrogen hyperfine coupling dominated the changes in the spectra as a function of rotation angle. The contributions from species 2, 3, and 4 were resolved at orientations of the crystal for which the spin-spin interaction for one of them was substantially greater or smaller than the spin-spin interaction for species 1. At most orientations of the crystal, two or more species gave overlapping lines, but the combined information from the three orthogonal planes required the presence of four species. Some discrepancies between the simulated and observed spectra suggested the presence of other species with lower populations or broader lines, but there was not sufficient information to adequately define these components.

Approximate nitroxyl g and A tensors were obtained by diagonalization of the data for species 1 in the three orthogonal planes. The values were refined by comparison of calculated and experimental spectra at selected orientations of the crystal at which the spectra were well resolved. All the species appeared to have about the same orientation of the nitroxyl z axis relative to the vanadyl axes. Small differences between the nitroxyl g and A values of the four species at some orientations of the crystal indicated that the alignments of

Table II. Orientation and Interaction Parameters^a

species	A_1^b	A_2^b	ϵ^b	η^b	r^c	J^d	pop. ^e	d_{\parallel}^d
1	158	92	82	-80	13.6	0	29	-20
2	158	92	54	-50	10.0	4	14	-52
3	158	92	66	-9	11.0	-3	7	-39
4	158	92	49	28	9.8	-2	7	-55
VO(TPP)							43	

^a Parameters are defined in Figure 1. ^b In units of degrees. ^c In units of Angstroms. ^d In units of 10^{-4} cm^{-1} . ^e In units of percent.

the nitroxyl z axis were not identical for the four species, but the differences were too small to adequately define. In the simulations it was assumed that the orientations of the g and A tensors were identical for the four species but that the value of A_{zz} was slightly larger for species 2 than for the other species. The principal values of the nitroxyl g and A tensors are given in Table I. The values are similar to those observed for spin-labeled copper complexes I and II and for other piperidiny nitroxyl radicals.⁶

The components of the g and A tensors for the vanadyl electron in spin-labeled complex III were estimated by diagonalization of the hyperfine splittings and g values as a function of orientation and were refined by computer simulation of the spectra. Data were also obtained for VO(TPP) doped into ZnTPP. Independent analysis of the data for VO(TPP) gave the same parameters as obtained for spin-labeled complex III. The values are given in Table I and are in good agreement with literature values: for VO(TPP) in frozen glasses $g_{\parallel} = 1.947-1.964$, $g_{\perp} = 1.984-1.989$, $A_{\parallel} = 157-161 \times 10^{-4} \text{ cm}^{-1}$, and $A_{\perp} = (52-57) \times 10^{-4} \text{ cm}^{-1}$,^{16,17} for VO(TPP) doped into a triphenylene single crystal $g_{\parallel} = 1.964$, $g_{\perp} = 1.985$, $A_{\parallel} = 159 \times 10^{-4} \text{ cm}^{-1}$, and $A_{\perp} = 55 \times 10^{-4} \text{ cm}^{-1}$.¹⁸ At most orientations of the crystal of VO(TPP)-doped ZnTPP, each vanadyl hyperfine line was split into a partially resolved nine-line pattern due to coupling to the four porphyrin nitrogens. In the simulations of the spectra, it was assumed that the four porphyrin nitrogens were equivalent. The apparent porphyrin nitrogen hyperfine splittings along the x , y , and z axes of the vanadyl hyperfine tensor were 2.3, 2.3, and $2.6 \times 10^{-4} \text{ cm}^{-1}$, respectively. From ENDOR studies it is known that the nitrogen hyperfine tensor is anisotropic in the porphyrin plane.¹⁹ However, the EPR spectra were not well enough resolved to show that the porphyrin nitrogens were pairwise nonequivalent. The nitrogen hyperfine splittings observed for VO(TPP) doped into ZnTPP (Table I) are in good agreement with the values given in the literature for an ENDOR study of VO(TPP) in a frozen glass: out of plane component, $2.6 \times 10^{-4} \text{ cm}^{-1}$; average of the in-plane components, $2.3 \times 10^{-4} \text{ cm}^{-1}$.¹⁹

The observed spin-spin splittings for each of the species as a function of the orientation of the crystal in the magnetic field are shown in Figures 3-6 along with the computer simulations of these plots. The angles that define the orientation of the interspin vector relative to the vanadyl axes and the values of r and J for each of the species were obtained from the simulations of the plots and were refined by comparison of calculated and experimental spectra at selected orientations, which showed well-resolved spectra. The values of the orientation and interaction parameters are given in Table II. The uncertainties in the parameters are the following: angles, $\pm 5^\circ$; r , $\pm 0.5 \text{ \AA}$; J , $\pm 2 \times 10^{-4} \text{ cm}^{-1}$. The dipolar splitting when the magnetic field is parallel to the interspin vector (d_{\parallel}) is also given in Table II. Since the g anisotropy is small, $|d_{\parallel}|$ is the maximum dipolar splitting and d_{\perp} is equal to $-0.5*d_{\parallel}$.

(16) Kivelson, D.; Lee, S.-K. *J. Chem. Phys.* **1964**, *41*, 1896-1903.

(17) Sato, M.; Kwan, T. *Bull. Chem. Soc. Jpn.* **1974**, *47*, 1353-1357.

(18) Bohandy, J.; Kim, B. F.; Jen, C. K. *J. Magn. Reson.* **1974**, *15*, 420-426.

(19) Mulks, C. F.; van Willigen, H. *J. Phys. Chem.* **1981**, *85*, 1220-1224.

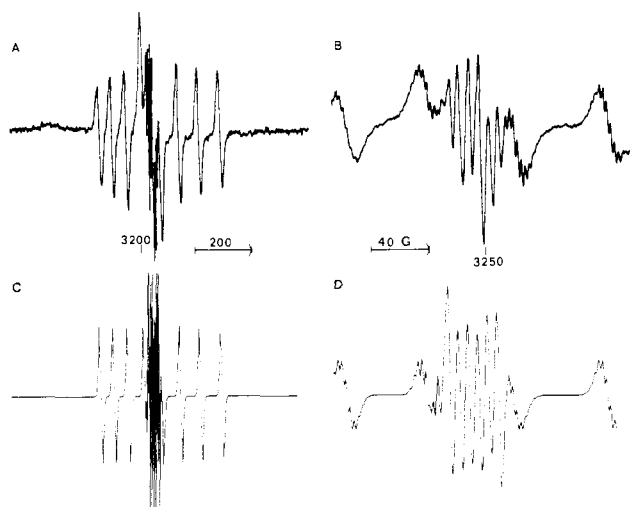


Figure 7. X-Band (9.110-GHz) EPR spectra of spin-labeled vanadyl complex III doped into ZnTPP obtained at $\theta = 90^\circ$ and $\phi = 90^\circ$: (A) 1000-G scan of the full spectrum obtained with 1.6-G modulation amplitude and 5-mW microwave power; (B) 200-G scan of the central region of the spectrum obtained with a gain setting 63% of that used in A; (C, D) corresponding calculated spectra.

Accurate determination of line widths was difficult due to the extensive overlap of the lines. Since there were vanadyl lines to both high field and low field of the nitroxyl lines and since J was small, the inner lines of part of the nitroxyl AB patterns were approximately on top of the outer lines of other nitroxyl AB patterns. Therefore, no attempt was made to distinguish between the line widths for the inner and outer lines. It was assumed that the three lines of a nitroxyl triplet had equal line widths. However, some of the simulations indicated that there were differences in the line widths within a triplet. It was also assumed that all the vanadyl lines had the same line width. This assumption gave good agreement between observed and calculated spectra for VO(TPP). However for spin-labeled complex III, the vanadyl line widths appeared to depend on the vanadyl nuclear spin state.

Results and Discussion

Figure 7 shows the EPR spectrum of III obtained for $\theta = 90^\circ$ and $\phi = 90^\circ$; i.e., the magnetic field was along the y axis. At this orientation, the vanadyl hyperfine splitting was about 60 G. The nitroxyl region of the spectrum was partially superimposed on the vanadyl lines with $m_I = \pm 1/2$ and was dominated by the lines from species 1. At this orientation, the nitroxyl nitrogen hyperfine splitting for species 1 was about 13.5 G and the spin-spin splitting was about 6 G, so the spectrum appeared to be six approximately equally spaced lines. The contributions from species 2, 3, and 4 were not well resolved at this orientation but were included in the simulations. In the 1000-G scan of the spectrum, it is evident that there is additional intensity that extends beyond the sharp nitroxyl lines that makes the vanadyl $m_I = \pm 1/2$ lines appear more intense than the other vanadyl lines in the spectrum. This intensity probably indicates the presence of other species in the crystal that have broad nitroxyl lines. They were not included in the simulations.

Figure 8 shows the EPR spectrum of III obtained for $\theta = 10^\circ$ and $\phi = 179^\circ$, i.e., the magnetic field was about 10° away from the z axis. At this orientation, the vanadyl hyperfine splitting was 169 G. The vanadyl $m_I = -1/2$ line was largely obscured by the sharper nitroxyl lines. In the nitroxyl region of the spectrum, the contributions from several of the species could be resolved. All of the species exhibited large nitrogen hyperfine splitting at this orientation of the crystal, which indicated that the nitroxyl z axes for all of the species were similarly oriented and near the vanadyl z axis. The nitrogen hyperfine splitting for species 1, 3, and 4 (24 G) was slightly smaller than for species 2 (26 G) at this orientation. Inspection

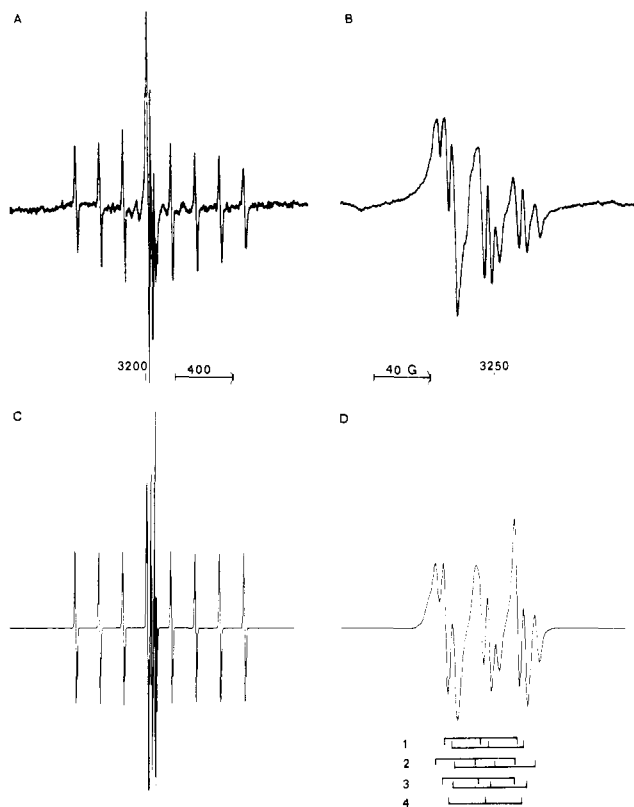


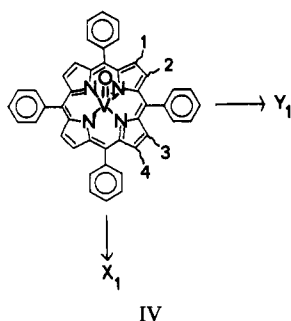
Figure 8. X-Band (9.107-GHz) EPR spectra of spin-labeled vanadyl complex III doped into ZnTPP obtained at $\theta = 10^\circ$ and $\phi = 179^\circ$: (A) 2000-G scan of the full spectrum obtained with 1.6-G modulation amplitude and 5-mW microwave power; (B) 200-G scan of the central region of the spectrum obtained with a gain setting 50% of that used in B; (C, D) corresponding calculated spectra.

of the values at other orientations indicated that the difference was due to a small difference in the values of A_{zz} rather than a difference in the orientations of the A tensors. The lines from species 1 were a sharp doublet of triplets. Since the spin-spin splitting for species 2 at this orientation was larger than the spin-spin splittings for the other species, its lines were the major contributions to the low-field and high-field portions of each of the components of the nitroxyl triplet. Species 3 and 4 had lower populations than species 1 and 2 and their lines were less well resolved at this orientation of the crystal. The crossover points for the lines from each of the species are indicated below the simulated spectrum.

In the simulated spectra, the intensity of the vanadyl lines relative to the nitroxyl lines was lower than in the experimental spectra. The agreement between observed and calculated spectra was improved by adding a 43% contribution from VO(TPP) that was not spin labeled. The crystal of III was grown from an analytically pure sample; however, it is possible that a small impurity of VO(TPP) may have preferentially doped into the host or that some hydrolysis of the spin-label linkage may have occurred during the long periods in solution that were required for crystal growth. There may also be some species present in the crystal for which the nitroxyl lines were broad. Since the vanadyl multiplets were much broader than the resolved nitroxyl lines, the omission of species with broad nitroxyl and/or vanadyl lines could perturb the apparent relative intensities of the nitroxyl and vanadyl lines.

When spin-labeled vanadyl porphyrin III is doped into a single crystal, the spin-labeled side chain could be located at any of the eight pyrrole carbons and could be oriented either above or below the porphyrin plane. Thus, there are 16 possible locations for the substituent. Locations that are related by rotation around the vanadyl z axis (the VO bond) or

by reflection in the porphyrin plane are distinguishable by EPR, but locations that are related by inversion are indistinguishable at all orientations of the crystal. In the crystal of III doped into ZnTPP, four distinct locations of the side chain were observed. The locations were characterized by different values of the angle parameters, ϵ and η . We have arbitrarily chosen to keep the values of η between $+90$ and -90° . When this was done, the values of ϵ fell between 0 and 90° . The values of η for the four species differ by increments of 30 – 40° , which is consistent with the angular increments expected for locations at successive pyrrole carbons around the porphyrin periphery. Since the vanadyl g and A tensors were axially symmetric, there was no molecular definition of the x and y axes. The x and y axes were arbitrarily defined relative to the faces of the crystal. Since the crystal structures of ZnTPP·THF and of VO(TPP) are not known, it is not possible to relate the arbitrary axis definitions to the true molecular axes. However, the relative locations of the four species can be viewed as in IV, recognizing that the values of η are relative to an arbitrary y axis.



The values of r obtained for III ranged from 9.8 to 13.6 \AA , with the larger values of r occurring for larger values of ϵ . A similar correlation between the values of r and ϵ was observed for copper complexes I and II.⁸ Inspection of molecular models indicated that if the conformations of the spin labels were approximately constant, the values of r and ϵ both increased as the whole side chain was forced toward the porphyrin plane. For species 2, 3, and 4 of vanadyl complex III, the values of r and ϵ were in the same range as those observed for species 1, 2, and 3 of copper complex II.⁸ For about the same values of r , the values of ϵ for vanadyl complex III were larger than for the analogous copper complex II.⁸ Alternatively, if similar values of ϵ were compared, the values of r were shorter for the vanadyl complex than for the copper complex. In the crystal structure of vanadyl octaethylporphyrin, it was observed that the vanadium atom is 0.54 \AA above the mean plane of the porphyrin toward the vanadyl oxygen.²⁰ If the conformations of the spin-labeled side chain were about the same for copper complex II and vanadyl complex III and the vanadyl ion was

above the porphyrin plane, the side chains on the same side of the plane should give smaller values of r and larger values of ϵ for the vanadyl complex than for the copper complex. Side chains on the opposite side of the plane from the vanadyl oxygen would be expected to have larger values of r and smaller values of ϵ for vanadyl than for copper. The data for III suggest that the side chains for species 1–4 were all on the same side of the porphyrin plane as the vanadyl oxygen. Such preferential orientation might arise from crystal-packing effects. The spatial requirements of the vanadyl oxygen might create a larger pocket on that side of the plane into which the side chain could fit than was available on the other side of the molecule. Since the crystals were grown from THF solution, there may be a THF molecule coordinated trans to the vanadyl oxygen. The spatial requirements of the axial ligand might make it more difficult to accommodate the side chains on the THF side of the porphyrin plane. Without crystallographic data, it is difficult to assess the validity of either of these proposals. The values of r for these complexes were sufficiently large that the expected effect of the metal displacement on the values of r and ϵ is small. It is also possible that systematic differences in the conformation of the side chains could be responsible for the differences in the values of r and ϵ for complexes II and III.

For the four conformations of III, the values of the exchange coupling constant, J , were between $+4$ and $-3 \times 10^{-4} \text{ cm}^{-1}$. These small values are consistent with the observation that in fluid solution the exchange interaction was less than the line widths of the nitroxyl lines.¹⁰ In the analogous cis isomer of the copper complex II, the values of J were between $+10$ and $-4 \times 10^{-4} \text{ cm}^{-1}$.⁸ Thus for the cis isomers II and III, the values of J were small and had both positive and negative signs. For trans isomer I all the major species had larger negative values of J . The data obtained for the vanadyl complex are consistent with our previous arguments concerning the analogy between electron–electron coupling constants and NMR nuclear–nuclear coupling constants.⁸

Conclusions

Single-crystal EPR spectra of III doped into ZnTPP indicated the presence of four conformations of the molecule in the crystal. The interspin distances for the four conformations were between 9.8 and 13.6 \AA . The electron–electron spin–spin coupling constants were between $+4$ and $-3 \times 10^{-4} \text{ cm}^{-1}$. There was no correlation between the values of r and J . The small values of J were in good agreement with the values obtained in fluid solution. Comparison of the values of r and ϵ for copper complex II and vanadyl complex III suggested that the spin-label side chains in III were on the same side of the porphyrin plane as the vanadyl oxygen.

Acknowledgment. This work was supported in part by NIH Grant No. GM21156.

Registry No. III, 76496-72-5; VO(TPP), 14705-63-6; ZnTPP, 14074-80-7.